2013

Magnetorheological elastomers and their applications

W H. Li
University of Wollongong, weihuali@uow.edu.au

X Z. Zhang
University of Wollongong

H Du
University of Wollongong, hdu@uow.edu.au

Magnetorheological elastomers and their applications

Abstract

Magnetorheological elastomers (MRE) are smart materials whose modulus or mechanical performances can be controlled by an external magnetic field. In this chapter, the current research on the MRE materials fabrication, performance characterisation, modelling and applications is reviewed and discussed. Either anistropic or isotropic or MRE materials are fabricated by different curing conditions where magnetic field is applied or not. Anistropic MREs exhibit higher MR effects than isotropic MREs. Both steady-state and dynamic performances were studied through both experimental and theoretical approaches. The modelling approaches were developed to predict mechanical performances of MREs with both simple and complex structures. The sensing capabilities of MREs under different loading conditions were also investigated. The review also includes recent representative MRE applications such as adaptive tuned vibration absorbers and novel force sensors.

Keywords

applications, magnetorheological, elastomers, their

Disciplines

Engineering | Science and Technology Studies

Publication Details

Li, W. H., Zhang, X. Z. & Du, H. (2013). Magnetorheological elastomers and their applications. In P. M. Visakh, S. Thomas, A. K. Chandra & A. P. Mathew (Eds.), Advances in Elastomers I: Blends and Interpenetrating Networks (pp. 357-374). Berlin, Germany: Springer.

Magnetorheological Elastomers and Their Applications

W.H.Li[1], X.Z. Zhang[1], and H. Du[2]

[1]*School of Mechanical, Materials & Mechatronic Engineering, University of Wollongong, Wollongong, NSW 2522, Australia*

[2]*School of Electrical, Computer & Telecommunications Engineering, University of Wollongong, Wollongong, NSW 2522, Australia*

1.Introduction to magnetorheological materials

Magnetorheological (MR) material is a class of smart materials whose rheological properties can be controlled rapidly and reversibly by the application of an external magnetic field. Traditionally, it is composed of MR fluids and MR foams, while Magnetorheological elastomers (MREs) became a new branch of this kind of smart material. MR materials typically consist of micron-sized magnetic particles suspended in a non-magnetic matrix [1]. In MR fluids, magnetic particles, such as iron or carbonyl iron particles, are suspended in a liquid carrier fluid. MR foams, in which the controllable fluid is contained in an absorptive matrix or magnetic particles are dispersed in a foam-like matrix, are solid-state materials with very low intrinsic modulus [1]. MREs are composites where magnetic particles are suspended in a non-magnetic solid or gel-like matrix. The particles inside the elastomer can be homogeneously distributed or they can be grouped (e.g. into chain-like columnar structures). To produce an aligned particle structure, the magnetic field is applied to the polymer composite during crosslinking so that the columnar structures can form and become locked in place upon the final cure [2-10].

The magnetic interactions between particles in these composites depend on the magnetization orientation of each particle and on their spatial relationship, coupling the magnetic and strain fields in these materials and giving rise to a number of interesting magneto-mechanical phenomena. For example, Shiga et al [2] prepared a kind of composite gel with magnetic properties. Then, Jolly et al. [3] tested and analysis the mechanical properties of silicon rubber based magnetorheological elastomer. When the magnetic field was 0.8T, the shear modulus ratio increased about 40% of the initial value. A number of groups have studied the effect of volume fraction on the MR effect and concluded the optimal volume fraction is around 27% [4-7]. Bossis et al. [8] investigated the electromagnetic, optical and other physical properties of MR elastomers. Lokander and Stenberg [9,10] prepared isotropic MR elastomres and investigated their magnetic, mechanical properties and their oxidation resistance, chemical and physical stability.

Although MR materials have many analogical mechanical behaviors, MREs have a unique mechanical performance different from others material: MREs have a controllable, field-dependent modulus while MR fluids and MR foam have a field-dependent yield stress.

This makes the two groups of materials complementary rather than competitive to each other. In other words, the strength of MR fluids is characterized by their field dependent yield stress while the strength of MREs is typically characterized by their field dependent modulus. The unique mechanism difference of MR fluids and MREs have made them to find different applications. MR fluids are widely used to develop semi-active damping devices, such as dampers, clutches and brakes [1]. MREs have found applications in developing adaptive tuned vibration absorbers [11-15].

In addition, MRE exhibits other obvious advantages: the particles in MREs are not able to settle with time and thus that there is no need for containers to keep the MR material in place; the response time of MREs is very short (several milli-seconds) because the particles, locked in the matrix, have no time to arrange again while MREs are applied an external magnetic field. All these characteristics have made MREs have a huge market potential.

2. Fabrication of isotropic and anistropic MR elastomers

There are two main types of MREs: isotropic and anistropic. The fabrication of these two kinds of MREs depends on whether an external magnetic field is applied or not. Fig. 1 is a schematic of the fabrication methods.

Fig. 1. Schematic of fabrication of both isotropic and anistropic MREs.

The anistropic MRE is a kind of pre-structured magnetic elastomer. It is the main investigated MREs in the literature. During the curing process, an external magnetic field is applied to the mixture of elastomer matrix and magnetic particles. Before the matrix iss not cured yet, the magnetic particles in the liquid still can move. They are able to align in the direction of magnetic field to form a chain-like or column structure (see Fig. 2a). After curing, these structures were locked in the matrix. Therefore, pre-structured MRE (also known as prepared under a magnetic field MR elastomer) is an anisotropic MR elastomer.

The isotropic MR elastomre is a kind of unstructured magnetic elastomers. During the

curing, No external magnetic field was applied on the mixture, and particles do not form chains or columnar structure (see Fig. 2b). Therefore unstructured MRE (also known as prepared without magnetic field MR elastomer) is an isotropic MRE.

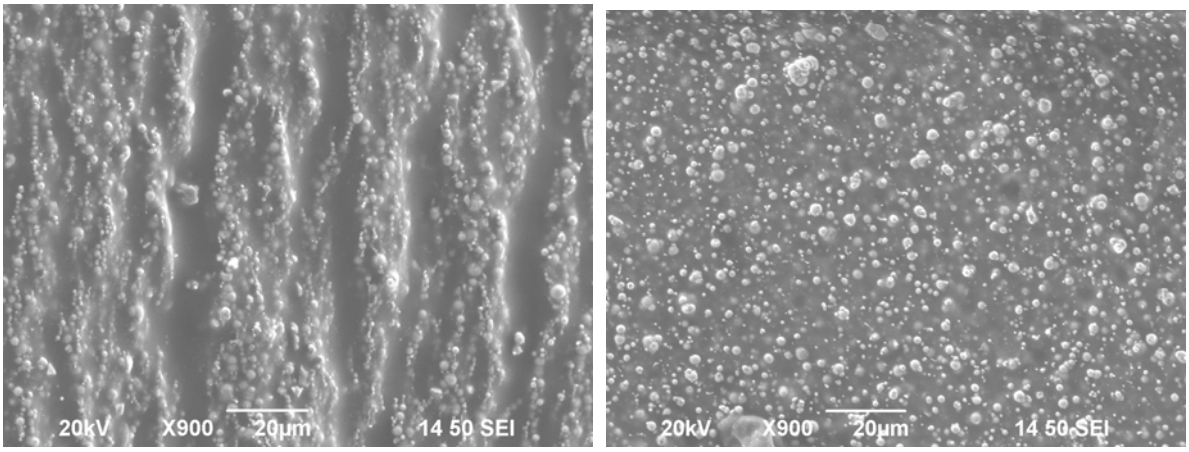

(a) (b)

Fig. 2. SEM images of MREs: (a) anistropic MRE; and (b) isotropic MRE [16].

Curing without magnetic field can greatly simplify the manufacture process, which is a significant advantage for manufacture in large quantities in industry [17-19]. However, the isotropic MREs only have about half field-dependant modulus compared with anisotropic MREs [19-21].

3. Steady-state and dynamic properties of MREs

3.1. Steady-state properties

The MR effect can be evaluated by measuring the shear strain-stress curve of sample with and without an applied magnetic field. The quasi-static shear method is generally employed to evaluate the shear modulus of MREs. Fig. 3 shows the strain-stress curve of a MRE sample at 7 different magnetic field intensity ranging from 0 mT to 750 mT with a magnetic field step increase of 125 mT. The slope of the strain-stress curve is the shear modulus of the material. As the figure shows, the shear modulus of the increased with the magnetic fields, proves that the MREs exhibited obvious MR effects. The shear stress shows a linear relationship with the shear strain when the strain is within 10%. This means the MRE acts with linear viscoelastic properties when the strain is below 10%. This finding is totally different from MR fluids where the linear viscoelastic region is only below 0.1% [22]. This also demonstrated that MREs generally operate at the pre-yield region while MRF operates at the post-yield region. When the strain is above 10% the modulus reaches a maximum value and then steadily decreases, which implies that MRE reaches nonlinear-viscoleastic regime.

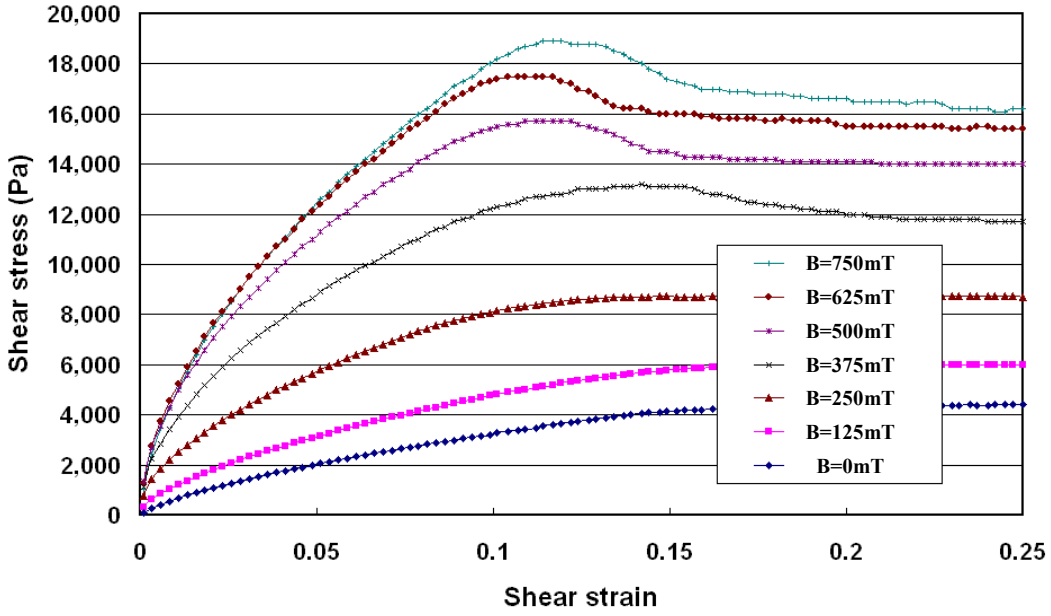

Fig. 3. Shear stress-strain curves of MRE sample under different magnetic fields.

3.2. Dynamic properties

Under dynamic loading, MREs exhibit viscoelastic properties. In our experimental study [23], harmonic loadings with various strain amplitudes ranging from 1% to 50%, and frequencies from 1 Hz to 10 Hz, were used to study dynamic properties of MRE samples. Fig. 4 shows the stress-strain relationships of the MRE sample at a constant strain amplitude of 10% but at various magnetic fields from 0 mT to 440 mT. It can be seen from this figure that all stresses and strains from nice elliptical shapes, the areas of which increase steadily with the increment of the magnetic fields. These results demonstrate that MRE materials have controllable mechanical properties. An increase in the stress-strain loop area with the magnetic field demonstrates that the damping capacity of the MR elastomers is a function of the applied magnetic field. These experimental results demonstrate that not only are the areas dependent on the magnetic fields, the shape of the ellipse loops are also different. In particular, the slope of the main axis of the elliptical loops varies with the magnetic field, which means that the modulus of MREs varies with magnetic field. Therefore, MREs exhibit variable stiffness and damping properties. This feature is totally different from ER and MR fluids, which mainly exhibit damping controllable properties.

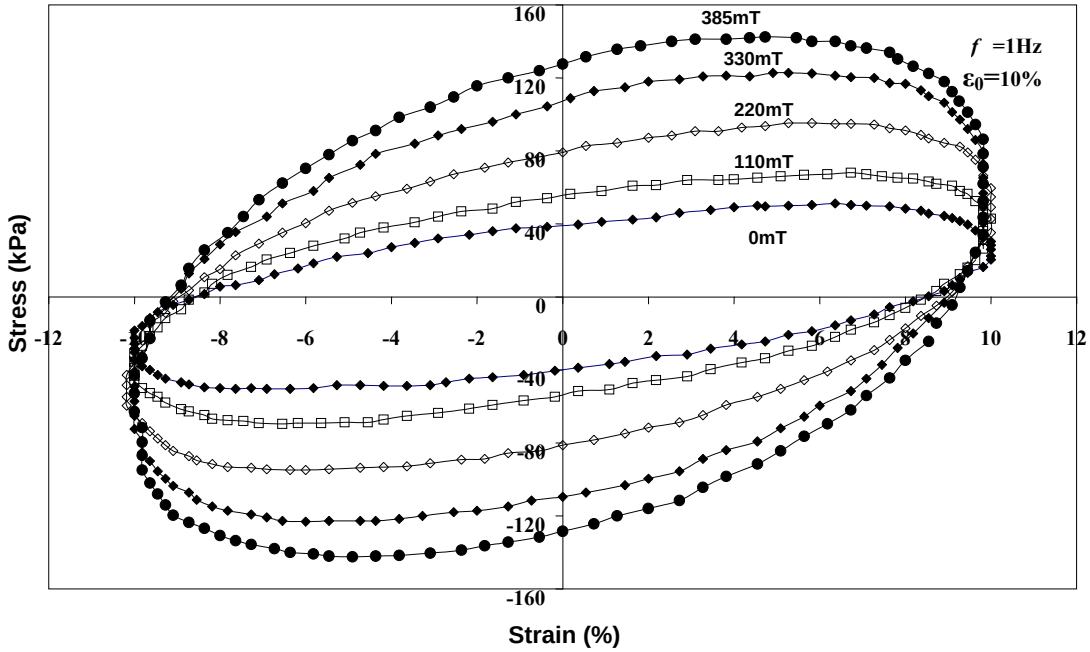

Fig. 4. Stress-Strain relationships with various magnetic fields at a constant strain amplitude of 10% [23].

Fig. 5 shows the effects of shear strain frequency inputs on MRE performance. The slope of the main axis of the elliptical loops increased with an increasing shear strain frequency inputs while the maximum stress amplitudes of different strain frequency inputs changed steadily. The shear strain frequency inputs mainly influences the slope of main axis of the ellipses. When the strain frequency inputs change from 1Hz to 5Hz, the slope of the main axis increases steadily. When the strain frequency inputs change from 5Hz to 10Hz, the slope of the main axis increases slightly. This implies that the stiffness of the system shows a slowly increasing trend with the frequency.

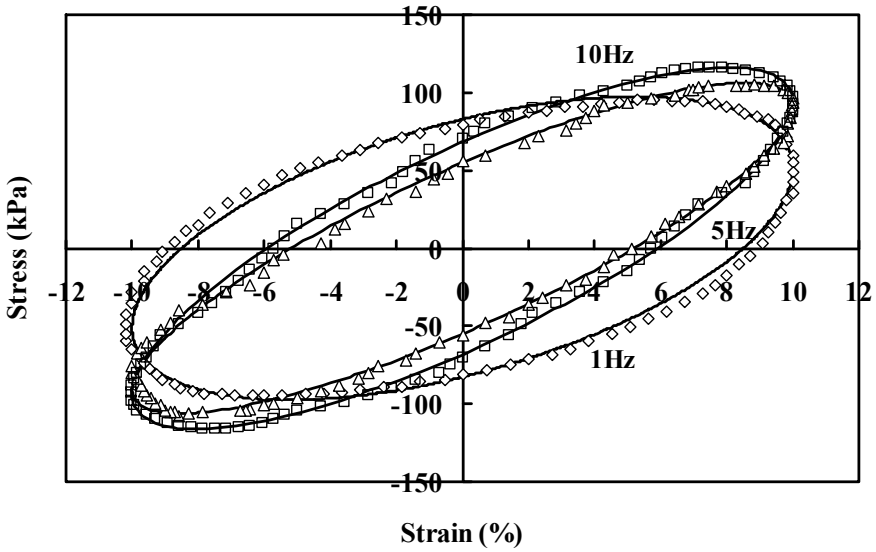

Fig. 5. Stress-Strain relationships for different frequency inputs in 220 mT [23].

3.3. MRE modeling

A number of non-parametric and parametric models have been developed to describe MREs performances. Jolly et al. [24] proposed a quasi-static model to explain the modulus increase by calculating the magnetic interaction between the adjacent particles. Davis [25] used finite element methods to analyze the modulus increase under varied magnetic fields. Shen et al.[26] developed a model that takes into account the magnetic interactions of dipoles in the same chain and the nonlinear properties of the host composites. Most of models are based on the basis of the dipole model for particle energy interaction, and they have the assumption that the particles are the same size and shape. These models are based on the previous studies on MR fluids and particle chains structure. Their results showed that the field-dependent modulus of MREs varies with the square of the saturation magnetization of the particles. Zhang et al. [27] analyzed the complex structure with different size particles or coating particles. The saturation of MREs has also been taken into account. Their theoretical and experimental results indicated that the MREs fabricated with particles have different sizes can provide larger field-dependent modulus.

Recently, we developed a parametric model to describe MRE dynamical performances. The experimental results, shown in Figures 4 and 5, indicate that the response stresses and input strains formed perfect elliptical loops when the strain amplitude is not above 10% and the excitation frequency is lower than 10 Hz. These results demonstrate that the MREs behave as linear viscoelastic properties. Viscoelastic properties of MR fluids have obtained intensive studies through experimental and modeling approaches [28,29]. In particular, a classical Kelvin-Voigt model and three-parameter standard solid model were used to model MR fluids at pre-yield region. Such linear viscoelastic model was mainly developed to process damping capabilities of ER and MR fluids. Compared with MR fluids, the MRE material exhibits a feature that its modulus and damping capability are both field dependent. To predict these characteristics, a four-parameter viscoelastic model, as shown in Fig. 6 was proposed by

extending the classical three-parameter standard solid model. In this model, a spring element is introduced, which is in parallel with the standard model, for representing the field dependence of modulus.

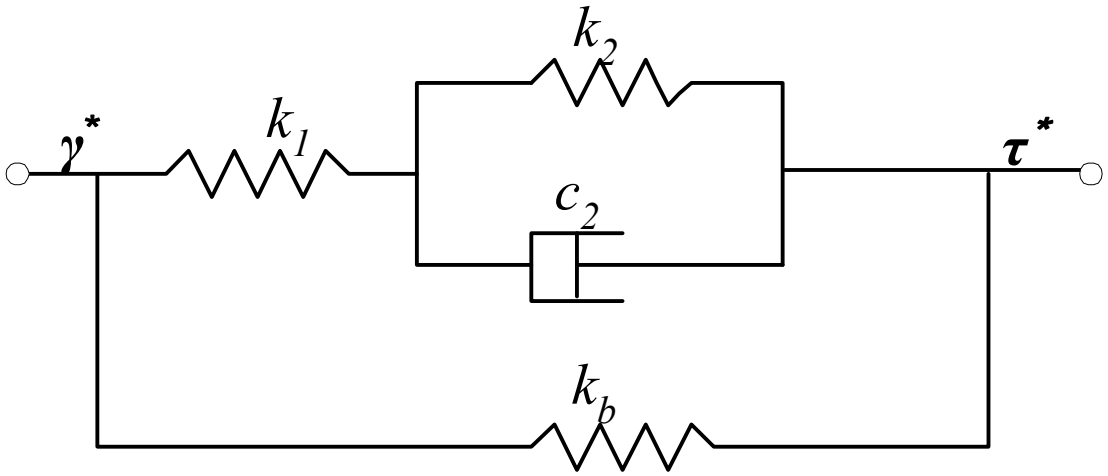

Fig. 6. Four-parameter viscoelastic model for MR elastomers.

In this model, k_1, k_2, and C_2 form a standard visocoelastic solid model, which mainly deals with the damping capabilities of the model, while k_b represents the field dependence of modulus. Suppose the input complex strain is γ^* while the output complex stress is τ^*, and the complex modulus is G^*, the stress-strain relationship is given by

$$\tau^* = G^*\gamma^* = (G_1 + iG_2)\gamma^* \tag{1}$$

where G_1 and G_2 are real and imaginary parts of the complex modulus, respectively. They can be derived by using the theory of linear viscoelasticity.

$$G_1 = \frac{(k_1k_b + k_2k_b + k_1k_2)[(k_1+k_2)^2 + c_2^2\omega^2] + c_2^2\omega^2k_1^2}{(k_1+k_2)[(k_1+k_2)^2 + c_2^2\omega^2]} \tag{2}$$

$$G_2 = \frac{c_2\omega k_1^2}{[(k_1+k_2)^2 + c_2^2\omega^2]} \tag{3}$$

where ω is the driving frequency.
Suppose that the shear strain input γ is a harmonic input

$$\gamma(t) = \gamma_0 \sin(\omega t) \tag{4}$$

The steady-state response of the stress can be obtained as

$$\tau(t) = \gamma_0\sqrt{G_1^2 + G_2^2}\sin(\omega t + \phi) \tag{5}$$

where ϕ is the phase angle difference between the input and output, which can be calculated as $\phi = \tan^{-1}(G_2/G_1)$.

The developed viscoelastic model includes four parameters, i.e. k_b, k_1, k_2, c_2. The model uses

the shear strain as an input, calculates the modulus G_1 and G_2 needed for the model, and then gives the shear stress, given by the equation (5). The four parameters are estimated on the base of the least squares method to minimise the error between the model-predicted stress and the experimental result. Using the parameters estimated from the system identification process, the stress versus strain was reconstructed and compared with the experimental data curve. Fig. 7 shows the reconstructed stress versus strain loops compared with the practical experimental curves. It can be seen from the plots that the model can simulate the experimental data very well.

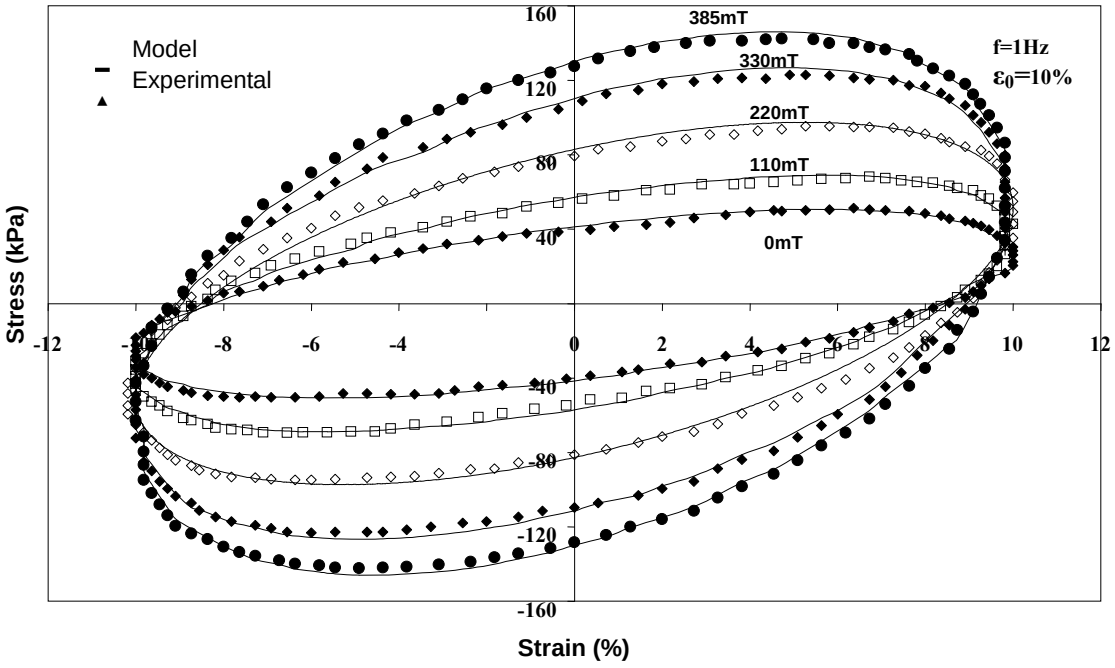

Fig. 7. A comparison between experimental data with model-predicted results with the amplitude input of 10%.

4. Sensing properties of MREs

4.1 MRE resistances

Unlike the study of MR effect of MREs, the research on MRE's sensing capabilities is quite few. MREs are generally insulating materials, the resistances of which are quite high. However, the MRE resistance value is dependent on the deformation strain and applied magnetic field. Bossis et al [8] found that the MRE resistance can have a huge resistance drop by five orders of magnitude when the magnetic field had a decrease of 6000 Oersted. Following this research, a number of groups have reported the sensing capabilities of different MRE materials. Kchit and Bossis [30] found that the initial resistivity of metal powder at zero pressure is about 108 Ωcm for pure nickel powder and 106 Ωcm for silver coated nickel particles. The change in resistance with pressure was found to be an order of magnitude larger for a MRE composite than for the same volume fraction of fillers dispersed randomly in the polymer. Wang et al. [31] proposed a phenomenological model to understand the impedance response of MREs under mechanical loads and magnetic fields. Their results showed that

MRE samples exhibit significant changes in measured values of impedance and resistance in response to compressive deformation, as well as applied magnetic field. Bica [32] found that MRE with graphite micro particles (~14%) is electroconductive. The magnetoresistance has an electric resistance whose value diminishes with both the increase of the intensity of the magnetic field and with the compression force. The variation of resistance with magnetic field intensity is due to the compression of MRE with graphite microparticles. In the approximation of the perfect elastic body, the sums of the main deformations and the compressibility module of MRE with graphite microparticles, depend on the magnetic field intensity. In our study [33], graphite was introduced into conventional MREs to change the overall resistances so that it can be detected by a multimeter. We found a MRE sample with 55% carbonyl iron, 20% silicon rubber and 25% graphite powder has the best performance. The test result showed that at a normal force of 5 N, the resistance decreases from 4.62 kΩ without a magnetic field to 1.78 kΩ at a magnetic field of 600 mT. The decreasing rate is more than 60%. This result also demonstrated the possibility of using MREs to develop a sensor for measuring magnetic fields. This result indicates that the detection is very sensitive to the normal force. When the normal force is 15N, the field-induced resistance only has less than 28% change from 0.65 kΩ at 0 mT to 0.47 kΩ at 600 mT.

4.2 Modeling approach

Depending on an elastic-plastic asperity microcontact model for contact between two nominally flat surfaces, Kchit and Bossis developed a model to analyse the contact of two rough surfaces. They used two kinds of magnetic particles: nickel and nickel coated with silver, dispersed in a silicone polymer as the polarised particles [30]. To understand the complex conductivity of particle embedded composites, quantitative or semi-quantitative models were developed by Zhao et al. [34]. The Maxwell–Wagner and the Bruggeman symmetric and asymmetric media equations were introduced by McLachlan [35] to model the electrical behaviour of conductor-insulator composites. The microstructures for which these effective media equations apply are considered in simulating the measured impedance and modular spectra of these composites. Woo et al. [36] developed a universal equivalent circuit model in modelling the impedance response of composites with insulating or conductive particles or fibres. Based on the microstructure of MREs, Wang et al. proposed an equivalent circuit model to interpret the impedance measurement results [31].

By supposing the anisotropic MRE has a single chain structure, a representative volume unit (RVU) as shown in Fig. 8, which consists of two neighboring hemispheres and the surrounding polymer metrix, is used to derive currents passing through the particles. Most of the current flowing through the RVU concentrates on the small area between the two adjacent hemispheres. Meanwhile the conductivity of the iron particles is much higher than that of the polymer therefore the electric potential drops on the particles could also be negligible. The insulating polymer film between two neighbouring iron particles is very thin because of the magnetic attraction during preparation and it is across this film that the electrical field assisted tunnel current can occur. The Fowler-Nordheim equation [37,38] can be used to express the tunnel current. Meanwhile the iron particles dispersing in the polymer matrix contribute to the conductivity of the polymer and then the total current density is the sum of the tunnel density j_t and the conduction density j_c, or

$$j = j_t + j_c = \alpha E_{loc}^2 \exp\left(-\frac{\beta}{E_{loc}}\right) + \sigma_f E_{loc} \tag{6}$$

in which σ_f is the conductivity of the polymer film.

The total current density j is for the current flowing through the small area between the tips of two adjacent iron particles, however, the density of RVU j_r should be derived from its cross section. So from the total density of RVU j_r and the electric field intensity E, the conductivity of typical MRE σ_r can be represented as

$$\sigma_r = \frac{j_r}{E} = \frac{\pi \cdot r_i^{\,2} \cdot j}{S_r \cdot E} = 3\phi \cdot r_i^{\,2} \left[\frac{2\alpha}{h^2} E \exp\left(-\frac{h\beta}{2r_p E}\right) + \frac{\sigma_f}{r_p h}\right] \tag{7}$$

in which the r_i is the radius of the area between the two adjacent iron particles

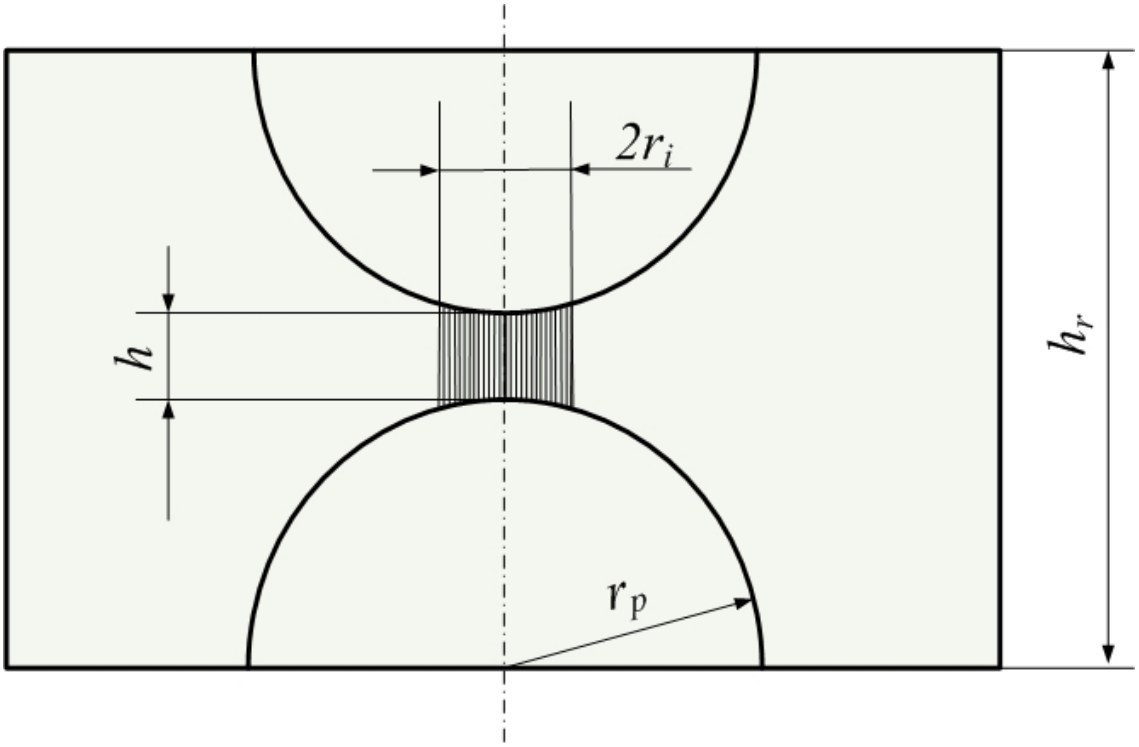

Fig. 8. The longitudinal section of RVU.

When a MRE sample is compressed its conductivity increases. This phenomenon is explained by two factors, one of which is the increments of the conductive area induced by the deformation of MREs and the other is the reduction of the thickness of the polymer membrane between the two adjacent iron particles.

From the Hertz Theory [39,40], when the initial compressed stress applied on MRE is σ_0, corresponding to which there is an initial contact area radius r_{i0}

$$r_{i0} = \left[\frac{3\pi\sigma_0\left(1-\nu^2\right)}{2E_p}\right]^{1/3} \cdot r_p \tag{8}$$

So the radius r_i increases along with the increment of compressed stress

$$r_i = r_{i0} + r_p\left(\left(\sigma_0 + \sigma\right)^{1/3} - {\sigma_0}^{1/3}\right)\cdot\left(\frac{3\pi\left(1-\nu^2\right)}{2E_p}\right)^{1/3} \tag{9}$$

Meanwhile the magnetic field also contributes to the resistance of MREs. When the external magnetic field is applied to MREs, the carbonyl iron particles are attracted by the poles of magnetic field. The nearer magnetic pole contributes much more powerful magnetic force than the other pole. So the attraction from the farther magnetic pole can be negligible.

For the two iron particles in each RVU, the magnetic attraction from the pole applied to the father particle compresses the thin film between the two adjacent iron particles. Similar to the piezoresistivity, the increment of the conductive area is the main cause for the conductivity increasing.

Thus, the radius r_i can be updated as

$$r_i = r_{i0} + r_p\left(\left(\sigma_0 + \sigma_1 + \sigma_2\right)^{1/3} - {\sigma_0}^{1/3}\right)\cdot\left(\frac{3\pi\left(1-\nu^2\right)}{2E_p}\right)^{1/3} \tag{10}$$

in which, σ_1 is the compressive stress , σ_2 is the stress from the magnetic attraction.

So the dependence of the conductivity of MREs on electric field intensity and compressive stress is

$$\sigma_m = 3\phi\cdot\left[\frac{2\alpha}{h^2}E\exp\left(-\frac{h\beta}{2r_pE}\right)+\frac{\sigma_f}{r_ph}\right]\cdot\left[r_{i0} + r_p\left(\left(\sigma_0 + \sigma_1 + \sigma_2\right)^{1/3} - {\sigma_0}^{1/3}\right)\cdot\left(\frac{3\pi\left(1-\nu^2\right)}{2E_p}\right)\right]^2 \tag{11}$$

When the initial condition σ_0 and r_{i0} are set, except E and σ the other parameters in this equation are all constants. So the conductivity of MREs σ_m is dependant on the intensity of the electric field E and the compressed stress σ.

For our fabricated graphite MRE based samples, the final resistance is given by

$$R_g = \lambda_g\lambda_i R = \frac{\lambda_g\lambda_i\rho l}{A} = \frac{\lambda_g\lambda_i l}{A\sigma_m}$$

$$= \frac{\lambda_g\lambda_i l}{3A\phi\cdot\left[\frac{2\alpha}{h^2}E\exp\left(-\frac{h\beta}{2r_pE}\right)+\frac{\sigma_f}{r_ph}\right]\cdot\left[r_{i0} + r_p\left(\left(\sigma_0 + \sigma_1 + \sigma_2\right)^{1/3} - {\sigma_0}^{1/3}\right)\cdot\left(\frac{3\pi\left(1-\nu^2\right)}{2E_p}\right)\right]} \tag{12}$$

The comparison between experimental results and modelling predictions is shown in Fig. 9. Though they couldn't match each other perfectly, still the trends of both the experimental result and the theoretical result are the same.

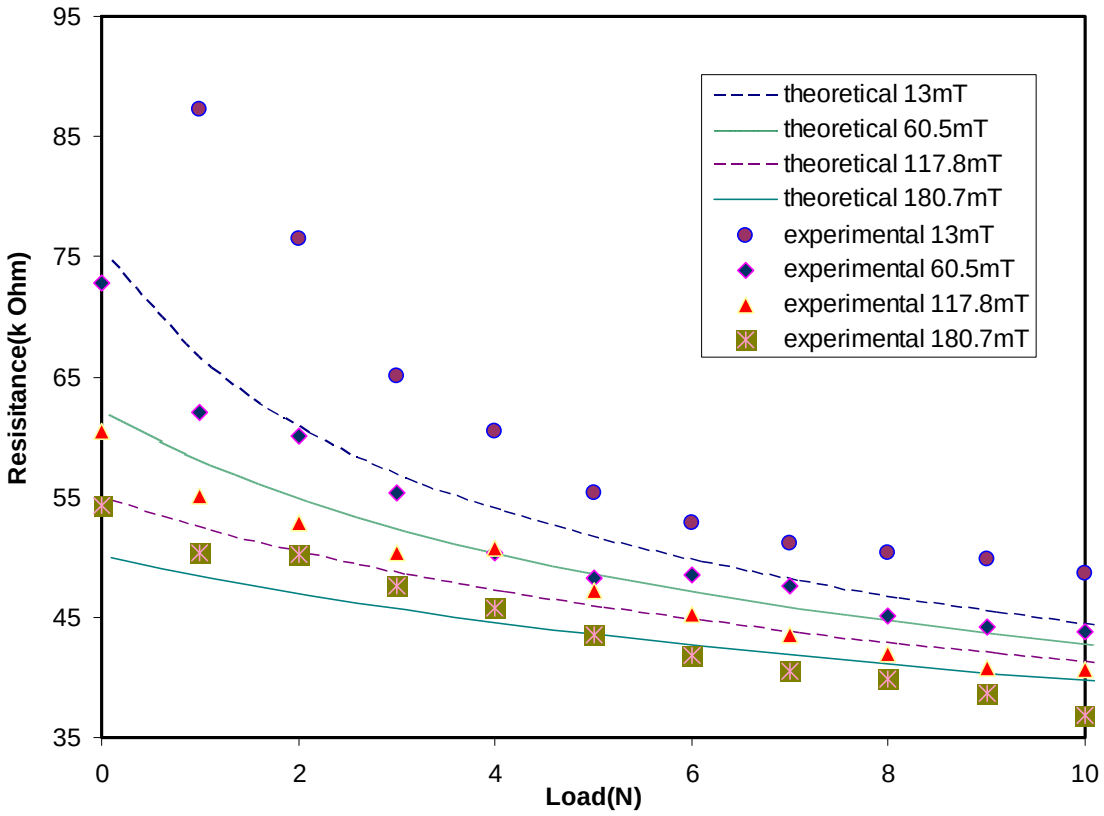

Fig. 9. Comparison between experimental result and theoretical result (anisotropic MRE Gr 21.95%)

5. MRE applications

5.1. Tunable dynamic vibration absorbers

MREs hold promise in enabling simple variable stiffness devices. The pioneering application of MREs was presented in vehicle industry. In US Patent 5816587 [41], as shown in Figure 10, a novel method and apparatus for varying the stiffness of a suspension bushing having a MRE disposed therein was presented. This allows for improved customer satisfaction by reducing dissatisfaction associated with braking events, such as shudder, which can result in increased noise, vibration and harshness. It solves these problems by controlling relative displacements of a longitudinal suspension member relative to a chassis member in a motor vehicle. The control method is: communicating a brake actuation signal from a brake actuator to a suspension control module; determining from the brake actuation signal a desired suspension bushing stiffness and generating an electrical current in response thereto; and communicating the electrical current to an electrical coil operatively associated with the MRE, thereby generating a magnetic field so as to vary the stiffness characteristics of the

MRE in a way to reduce an operator's perception of brake induced shudder. As shown in Figure 10, the apparatus comprises a suspension bushing shaft, an inner steel cylinder annularly surrounding the suspension bushing shaft, a MRE annularly surrounding the annular inner steel cylinder, and an outer steel cylinder annularly surrounding the annular MRE. An annular coil is disposed about an outer peripheral surface portion of the annular inner steel cylinder so as to be interposed between the annular inner steel cylinder and the annular MRE, and the coil is adapted to be electrically connected to the automotive vehicle electrical system by means of suitable electrical leads. By applying suitable predetermined amounts of electrical current to the suspension bushing coil, a variable magnetic field is generated which variably controls the stiffness values of the suspension bushing. The suspension bushings stiffness can therefore be adjusted in response to actuation of the brake system to reduce brake shudder.

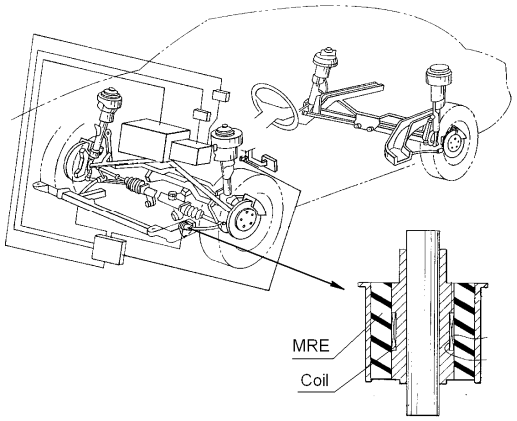

Figure 10. MREs suspension bushing [41].

In US Patent 7086507 and 20050011710 [42, 43], the inventors developed MRE devices and methods for their use for vibration isolation by changing the storage and loss modulii of one or more MRE layers. As shown in Figure 11, the MREs are sandwiched between magnetic activation layers. The magnetic activation layers contain embedded magnetic nodes that control the magnetic field, and thus the stiffness, of the MRE. The current and voltage supplied to the electromagnets will affect the magnetic field strength within the MRE and, hence, the stiffness of the MRE. The current and voltage are determined by the external vibration and associated forces imparted to the MRE device. This system can detect, measure and signal one or more physical manifestations of these external forces, and transforming this signal into the appropriate current and voltage to send to the magnets to obtain optimal vibration isolation energy dissipation for a given shock event. These MRE devices are used for vibration isolation of mechanical systems for random shock events.

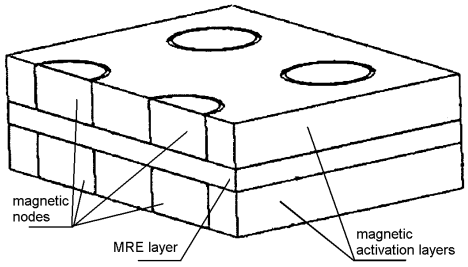

Figure 11. MRE devices for shock isolation [42,43]

MREs can also be used as the smart spring in dynamic vibration absorber. In US Patent 7102474 and 20050040922 [44, 45], the inventors presented an adaptive vibration absorbers (AVAs) working with MREs. As shown in Figure 12, the AVA is designed to operate selectively over a range of frequencies rather than a single frequency. It is configured of the elements including a base mass and an absorber mass connected by a pair of MREs, which function effectively as tunable springs and are also held responsible for the advantageous bandwidth increase in vibration suppression by the AVA. The configuration and composition of the elements of the exemplary AVA provide a path (also referred to as magnetic circuit) for magnetic flux that may be induced by a magnetic field source. Specifically, the magnetic circuit passes through MREs. When the source provides the magnetic field and flux travels through the described magnetic circuit, the change of MREs' properties will make the system's natural frequency shift. This change may be controlled as necessary or desired via a control algorithm applied through a processor. A number of research groups were focused on such applications, for example, Albanese [46] and Holdhusen [47] presented MRE absorbers working in a compression mode. Deng et al. [11,48], Zhang and Li [14] presented MRE absorbers worked in a shear mode. Their results indicated that the frequency of vibration absorber can be tuned in wide frequency range, and the controlled frequency band was expanded too.

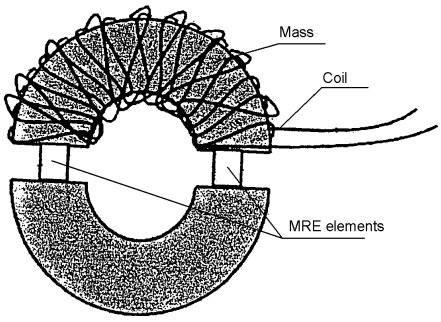

Figure 12. AVA having MRE elements [44,45]

5.2. MRE force sensors

Because of their magnetic field sensitive behavior, MREs were also considered as one of idea materials for sensor and actuator. In US Patent 5814999 [49], a method and apparatus for measuring displacement and force applied to an elastomeric body having a MRE disposed therein has been discovered. A transducer apparatus comprises two structural members and a MRE interposed between them. A module is provided for acquiring measurement data by applying a drive signal to an electrode disposed within the MRE and monitoring a preselected electrical state of the MRE. The module generates an output signal corresponding to variations the preselected electrical state caused by deflections of the MRE. It increases the usefulness of conventional elastomeric members by providing within them additional materials so that they may serve as transducers in addition to serving as isolators and pivotable joints, etc. This combination of functionality reduces part and assembly complexity as well as improving overall package efficiency for the assembled product.

6. Conclusions

This chapter presented a review of the state of the art in MREs technology. The basic materials, fabrication methods and many models to describe MREs' behavior were discussed. There is a growing need to understand and model their behavior and improve them by using optimal components and fabrication methods. The potential applications of this smart material were introduced. The patent review indicated that researchers continue to develop new MREs with new materials to meet new requirements. There were many applications prospect, which provide an impetus for continued research in this area. Numerous applications, which make use of controllable stiffness and the unique anisotropic characteristics of these elastomers, will be developed and the research efforts of the past decade in MREs will be paid off in the near future.

7. References

1. Carlson JD., Jolly MR. MR fluid, foam and elastomer devices. Mechatronics 2000; 10: 555–569.
2. Shiga T., Okada A., Kurauchi T. Magnetroviscoelastic behavior of composite gels. J. Applied Polymer Science 1995; 58: 787–792.
3. Jolly M.R., Carlson J.D., Munoz B.C., Bullions T.A. The magnetoviscoelastic response of elastomers composites consisting of ferrous particles embedded in a polymer matrix. Journal of Intelligent Material Systems and Structures, 7, 613–622, 1996.
4. Ginder JM., Clark SM., Schlotter WF., Nichols ME. Magnetostrictive phenomena in magnetorheological elastomers. Int. J. Modern Phys. B 2002; 16, Nos. 17&18: 2412–2418.
5. Zhou G.Y., Shear properties of a magnetorheological elastomer, Smart Materials & Structures, 12, 139-146, 2003.
6. Chen L., Gong, X.L., Jiang W.Q., et al., Investigation on magnetorheological elastomers based on natural rubber, Journal of Materials Science, 42, 5483-5489, 2007.
7. Hu Y., Wang Y.L., Gong X.L., et al. New magnetorheological elastomers based on polyurethane/Si-rubber hybrid, Polymer testing, 24, 324-329, 2005.
8. Bossis G., Abbo C., Cutillas S., et al. Electroactive and Electrostructured Elastomers. International Journal of Modern Physics B, 2001 15(6&7), 564-573.
9. Lokander M., Stenberg B. Performance of isotropic magnetorheological rubber materials. Polymer Testing 2003; 22: 245–251.
10. Lokander M., Stenberg B. Improving the magnetorheological effect in isotropic magnetorheological rubber materials. Polymer Testing 2003; 22: 677–680.
11. Deng H.X., Gong X.L., Wang L.H., Development of an adaptive tuned vibration absorber with magnetorheological elastomer, 15, Smart Materials & Structures, N111-N116, 2006.
12. Ni Z.C., Gong X.L., Li J.F., et al., Study on a dynamic stiffness-tuning absorber with squeeze-strain enhanced magnetorheological elastómer, Journal of Intelligent Material Systems & Structures, 20, 1195-1202, 2009.

13. Xu Z.B., Gong X.L., Liao G.J., et al., An active-damping-compensated magnetorheological elastomer adaptive tuned vibration absorber, Journal of Intelligent Material Systems & Structures, 21, 1039-1047, 2010.
14. Zhang X.Z., and Li W.H., "Adaptive Tuned Dynamic Vibration Absorbers Working with MR Elastomers", Smart Structures & Systems, 5 (5), 517-529, 2009.
15. Hoang N., Zhang N., Du H., An adaptive tunable vibration absorber using a new magnetorheological elastomer for vehicular powertrain transient vibration reduction, Smart Materials & Structures, 20 (2011) 015019.
16. Tian T.F., Li W.H., Alici G., et al., Microstructure and magnetorheology of graphite based MR elastomers, Rheologica Acta, print online, DOI: DOI) 10.1007/s00397-011-0567-9.
17. Lokander M., Stenberg B. Performance of isotropic magnetorheological rubber materials. Polymer Testing 2003; 22: 245–251.
18. Lokander M., Stenberg B. Improving the magnetorheological effect in isotropic magnetorheological rubber materials. Polymer Testing 2003; 22: 677–680.
19. Gong X.L., Zhang X.Z., Zhang P.Q., Fabrication and characterization of isotropic magnetorheological elastomers, Polymer Testing, 24, 669-676, 2005.
20. Davis LC., Model of magnetorheological elastomers. J. Applied Phys. 1999; 85(6): 3348–3351.
21. Ginder JM., Nichols ME., Elie LD., Clark SM. Controllable stiffness components based on magnetorheological elastomers. Smart Structures and Materials 2000: Smart Structures and Integrated Systems. Wereley, N.M. (Ed.). Proc. of SPIE 2000; 3985: 418–425.
22. Li W.H., Du H., Chen G., et al., Nonlinear Viscoelastic Properties of MR Fluids under Large-Amplitude Oscillatory Shear, Rheological Acta, 42 (3): 280-286, 2003.
23. Li W.H., Zhou Y., and Tian T.F., Viscoelastic Properties of MR Elastomers under Harmonic Loading, Rheologica Acta, 49, 733-740, 2010.
24. Jolly MR., Carlson JD., Munoz BC., A model of the behaviour of magnetorheological materials". Smart Mater. Struct. 1996; 5: 607–614.
25. Davis LC., Model of magnetorheological elastomers. J. Applied Phys. 1999; 85(6): 3348–3351.
26. Shen Y., Golnaraghi MF., Heppler GR. Experimental research and modeling of magnetorheological elastomers. J. Intelligent Material Systems and Structures 2004; 15: 27–35.
27. Zhang X.Z., Li W.H., Gong X.L. An effective permeability model to predict field-dependent modulus of magnetorheological elastomers. Communications in Nonlinear Science And Numerical Simulation 2008; 13(9): 1910-1916.
28. Li W.H., Du H., Chen G., et al., Nonlinear Viscoelastic Properties of MR Fluids under Large-Amplitude Oscillatory Shear", Rheological Acta, 42, 280-286, 2003.
29. Li W.H., Du H., Chen G., et al., Nonlinear Rheological Behavior of MR Fluids: Step Strain Experiments, Smart Materials and Structures, 11, 209-217, 2002.

30. Kchit N., and Bossis, G., Electrical resistivity mechanism in magnetorheological elastomer. Journal of Physics D-Applied Physics, 42(10): p. 5505-5505, 2009.
31. Wang X.J., Gordaninejad, F., Calgar, M., et al., Sensing Behavior of Magnetorheological Elastomers. Journal of Mechanical Design, 131(9): p. 6., 2009.
32. Bica I., Influence of the transverse magnetic field intensity upon the electric resistance of the magnetorheological elastomer containing graphite microparticles. Materials Letters, 63(26): p. 2230-2232, 2009.
33. Li W.H., Kostidis K., Zhang X.Z., et al., Development of a Force Sensor Working with MR Elastomers, in 2009 Ieee/Asme International Conference on Advanced Intelligent Mechatronics, Vols 1-3. 2009, Ieee: New York. p. 233-238, 2009.
34. Zhao, Y., Maietta, D.M. and Chang, L., 2000. An Asperity Microcontact Model Incorporating the Transition From Elastic Deformation to Fully Plastic Flow. Journal of Tribology, 122(1): p. 86-93.
35. McLachlan, D.S., 2000. Analytical functions for the dc and ac conductivity of conductor-insulator composites. Journal of Electroceramics, 5(2): p. 93-110.
36. Woo, L.Y., Wansom, S., Hixson, A.D., Campo, M.A. and Mason, T.O., 2003. A universal equivalent circuit model for the impedance response of composites. Journal of Materials Science, 38(10): p. 2265-2270.
37. Weinberg, Z.A., 1982. On tunneling in metal-oxide-silicon structures. Journal of Applied Physics, 53(7): p. 5052-5056.
38. Serdouk, S., Hayn, R. and Autran, J.L., 2007. Theory of spin-dependent tunneling current in ferromagnetic metal-oxide-silicon structures. Journal of Applied Physics, 102(11): p. 113707-1-113707-5.
39. Zhupanska, O.I. and Ulitko, A.F., 2005. Contact with friction of a rigid cylinder with an elastic half-space. Journal of the Mechanics and Physics of Solids, 53(5): p. 975-999.
40. Etsion, I., Levinson, O., Halperin, G. and Varenberg, M., 2005. Experimental investigation of the elastic-plastic contact area and static friction of a sphere on flat. Journal of Tribology, 127(1): p. 47-50.
41. Stewart WM. Ginder JM. Elie LD. Method and apparatus for reducing brake shudder. US Patent 5816587, 1998.
42. Hitchcock GH., Gordaninejad F. Fuchs A. Controllable magneto-rheological elastomer vibration isolator. US Patent 7086507, 2006.
43. Hitchcock GH., Gordaninejad F., Fuchs A. Controllable magneto-rheological elastomer vibration isolator. US Patent 20050011710, 2005.
44. Lerner AA., Cunefare KA. Adaptable vibration absorber employing a magnetorheological elastomer with variable gap length and methods and systems therefore. US Patent 7102474, 2006.
45. Lerner AA., Cunefare KA. Adaptable vibration absorber employing a magnetorheological elastomer with variable gap length and methods and systems therefore. US Patent 20050040922, 2005.
46. Albanese AM. The Design and Implementation of a Magnetorheological Silicone Composite State-Switched Absorber. A Thesis for the Degree Master of Science, Georgia Institute of Technology, August 2005.

47. Holdhusen MH.. The State-Switched Absorber Used for Vibration Control of Continuous Systems. A Dissertation for the Degree Doctor of Philosophy, Georgia Institute of Technology, February 2005.
48. Deng HX., Gong XL. Adaptive tuned vibration absorber based on magnetorheological elastomer, J. Intell. Mater. Sys. and Struct. 2007; 18(12): 1205-1210.
49. Elie LD., Ginder JM., Mark JS., Nichols ME. Method and apparatus for measuring displacement and force. US Patent 5814999, 1998.
50. Bellan C., Bossis G. Field dependence of viscoelastic properties of MR elastomers. Int. J. Modern Phys. B 2002; 16, Nos. 17&18: 2447–2453.
51. Horvath AT., Klingenberg DJ., Shkel YM. Determination of rheological and magnetic properties for magnetorheological composites via shear magnetization measurements. Int. J. Modern Phys. B 2002; 16, Nos. 17&18: 2690–2696.
52. Zhou G.Y., Complex shear modulus of a magnetorheological elastomer, Smart Materials & Structures, 13, 1203-1210, 2004.
53. Chen L., Gong X.L., Li W.H., Effect of carbon black on the mechanical performances of magnetorheological elastomers, Polymer testing, 27, 340-345, 2008.
54. Chen L., Gong X.L., Li W.H., Microstructures and viscoelastic properties of anisotropic magnetorheological elastomers, Smart Materials & Structures, 16, 2645-2650, 2007.
55. Demchuk SA., Kuzmin VA. Viscoelastic properties of magnetorheological elastomers in the regime of dynamic deformation. J. Engineering Physics and Thermophysics 2002; 75(2): 396–400.
56. Zhang W., Gong X.L., Jiang W.Q., et al., Investigation of the durability of anisotropic magnetorheological elastomers based on mixed rubber, Smart Materials & Structures, 19 (2010), 085008,